Relationship of Phospholipid Distribution to Shape Change in Ca^{2+}-Crenated and Recovered Human Erythrocytes†

Sansan Lin, Eungyeong Yang, and Wray H. Huestis*

Department of Chemistry, Stanford University, Stanford, California 94305

Received January 27, 1994; Revised Manuscript Received March 23, 1994®

ABSTRACT: Echinocytosis induced by elevation of intracellular Ca^{2+} in human erythrocytes can be reversed by removal of the cation. Using back-extraction of radiolabeled dilauroyl phospholipid analogs which had been incorporated into the cell membrane, we examined the relationship between this reversible shape transformation and phospholipid distribution. Upon Ca^{2+} crenation of cells, surface exposure of phosphatidylserine and phosphatidylethanolamine was observed simultaneously with inward diffusion of phosphatidylcholine. Removal of Ca^{2+} allowed resequestration of exposed phosphatidylserine to the membrane inner monolayer, but randomized phosphatidylethanolamine and phosphatidylcholine were not redistributed to their original states. Both shape reversion and retranslocation of phosphatidylserine were reversibly inhibited by vanadate. On the other hand, the cell shape recovery was found to be independent of membrane skeleton and phosphoinositide metabolism and was supported by ATP resynthesis only under conditions where the aminophospholipid translocator is active. Other Ca^{2+}-mediated biochemical changes, such as generation of diacylglycerol and fatty acids, were found to have no effect on Ca^{2+} crenation or its reversal, or upon transbilayer distribution of any phospholipid. These findings suggest that Ca^{2+} induces phospholipid redistribution, possibly by direct interaction with the lipid bilayer and, further, that metabolic recovery from Ca^{2+} crenation reflects selective retransport of phosphatidylserine to the membrane inner monolayer.

An increase in cytosolic Ca^{2+} concentration in human erythrocytes leads to a cell shape change from the normal biconcave discocyte to the crenated echinocyte, followed by release of microvesicles (White, 1974; Allan & Michell, 1975; Henseleit et al., 1990). Previous investigations on Ca^{2+}-induced microvesiculation have suggested that this membrane budding might be related to breakdown of polyphosphoinositides [phosphatidylinositol 4-phosphate (PIP)[1] and phosphatidylinositol 4,5-bisphosphate (PIP_2)] by a Ca^{2+}-activated phospholipase C (Allan & Michell, 1978; Ponnappa et al., 1980), since budding is not observed in species of erythrocytes lacking this lipase (Allan & Thomas, 1981; Raval & Allan, 1985). Ca^{2+}-induced cell crenation is reversible: on removal of Ca^{2+}, crenated cells incubated in supplemented buffer recover normal discoid shape (Anderson & Lovrien, 1981; Ferrell & Huestis, 1982; Whatmore et al., 1990). The mechanism of this shape reversion has not been examined extensively.

Similar cell shape changes, but mediated by metabolic conditions, have been shown to correlate with inositide phospholipid metabolism (Ferrell & Huestis, 1984). Cell crenation by metabolic depletion coincides with the phosphomonoesterase conversion of PIP_2 to PI and phosphatidic acid (PA) to diacylglycerol (DG). The resultant smaller head groups of PI and DG occupy a smaller area in the membrane inner monolayer, producing a bilayer imbalance that would be expected to yield echinocytic shape (Sheetz & Singer, 1974). When metabolically crenated cells are supplemented with nutrients to restore their ATP, cells recover discoid shape, with rephosphorylation of the lipids (Ferrell & Huestis, 1984). Complete regeneration of phosphoinositide populations is not possible in Ca^{2+}-crenated cells, since mature mammalian erythrocytes lack pathways for reversal of phosphodiesterase activity (Ponnappa et al., 1980). It has been suggested, however, that rephosphorylation of phosphatidylinositol (PI) may mediate shape reversal from Ca^{2+} crenation (Anderson, 1989).

Elevated cytosolic Ca^{2+} in erythrocytes also has been shown to induce transbilayer redistribution of the major phospholipids (Chandra et al., 1987; Comfurius et al., 1990b; Connor et al., 1990; Williamson et al., 1992): aminophospholipids [phosphatidylserine (PS) and phosphatidylethanolamine (PE)] normally confined in the membrane inner monolayer (Verkleij et al., 1973) were found to be partially exposed in the outer monolayer, while phosphatidylcholine (PC) and sphingomyelin (SM) were redistributed from the membrane outer monolayer to the inner monolayer. In platelets as well as red cells, it has been shown that the surface exposure of PS correlates in time with Ca^{2+}-induced microvesiculation (Sims et al., 1989; Comfurius et al., 1990b; Schroit & Zwaal, 1991; Zwaal et al., 1993), and removal of Ca^{2+} allows resequestration of exposed PS to the membrane inner monolayer in remnant cells (Comfurius et al., 1990b). The mechanism of Ca^{2+}-mediated phospholipid reorientation is poorly understood, and the possible relationship between phospholipid organization and cell shape has not been explored.

† This work was supported by NIH Grant HL 23787.

* To whom correspondence should be addressed.

® Abstract published in *Advance ACS Abstracts,* May 1, 1994.

[1] Abbreviations: ATP, adenosine triphosphate; BSA, bovine serine albumin; DG, diacylglycerol; DLPC, dilauroylphosphatidylcholine; DLPE, dilauroylphosphatidylethanolamine; DLPS, dilauroylphosphatidylserine; [^{14}C]DLPC, dilauroylphosphatidyl[1-^{14}C]choline; [^{14}C]DLPE, dilauroylphosphatidyl[2-^{14}C]ethanolamine; [^{3}H]DLPS, dilauroylphosphatidyl-L-[3-^{3}H]serine; DMSO, dimethyl sulfoxide; EDTA, ethylenediaminetetraacetic acid; EGTA, ethylene glycol bis(β-aminoethyl ether)-*N,N,N',N'*-tetraacetic acid; HCT, hematocrit; HEPES, *N*-(2-hydroxyethyl)piperazine-*N'*-2-ethanesulfonic acid; MI, morphological index; OAG, 1-oleoyl-2-acetyl-*sn*-glycerol; PA, phosphatidic acid; PC, phosphatidylcholine; PE, phosphatidylethanolamine; PI, phosphatidylinositol; PIP, phosphatidylinositol 4-phosphate; PIP_2, phosphatidylinositol 4,5-bisphosphate; PS, phosphatidylserine; SM, sphingomyelin; PMSF, phenylmethanesulfonyl fluoride; SDS, sodium dodecyl sulfate; TLC, thin-layer chromatography; Tris, tris(hydroxymethyl)aminomethane.

0006-2960/94/0433-7337$04.50/0

In the present work, we investigate the interrelationship between Ca^{2+}-induced changes in lipid metabolism and organization, and attendant cell shape changes. Radiolabeling results indicate that polyphosphoinositides are not regenerated by any mechanism during recovery from calcium crenation. Back-extraction of radiolabeled lipid analogs demonstrates that restoration of normal transbilayer lipid asymmetry is incomplete in recovered cells: among all phospholipids randomized in Ca^{2+}-crenated cells, only PS is retranslocated to the membrane inner monolayer in recovered cells. This PS resequestration correlates kinetically with cell shape reversal from crenation, and both events can be blocked by vanadate treatment. Possible mechanisms that might cause Ca^{2+}-mediated lipid reorientation also were examined.

MATERIALS AND METHODS

Materials. Dilauroylphosphatidylcholine (DLPC), dilauroylphosphatidylethanolamine (DLPE), bovine serum albumin (BSA, 96–99% albumin), 1-oleoyl-2-acetyl-*sn*-glycerol (OAG), palmitic acid, sodium orthovanadate, and phospholipase D (Type VII, from streptomyces species) were obtained from Sigma Chemical Co. (St. Louis, MO). L-[3-^{3}H]Serine (1 Ci/mol), [2-^{14}C]ethanolamine (54 Ci/mol), and [^{14}C]methyl iodide (6 Ci/mole) were purchased from Amersham Corp. (Arlington Heights, IL). [^{32}P]H_3PO_4 was purchased from NEN Research Products (Boston, MA). A23187 was purchased from Calbiochem (San Diego, CA). All other chemicals were of reagent grade.

Synthesis of Radiolabeled Phospholipids. [^{14}C]DLPC was synthesized from DLPE and methyl iodide (Aldrich) plus [^{14}C]methyl iodide, as described previously (Stockton et al., 1974; Ferrell et al., 1985). [^{3}H]DLPS was synthesized by phospholipase D-catalyzed head group exchange (Comfurius et al., 1990a) of DLPC with serine and L-[3-^{3}H]serine. [^{14}C]-DLPE synthesis was performed similarly by the head group exchange of DLPC with ethanolamine and [2-^{14}C]ethanolamine (Juneja et al., 1988). The reaction was carried out in buffered acetate/ethyl acetate (pH 5.6) at room temperature, and its progress was monitored by thin-layer chromatography (TLC). When most of the PC was converted to PE (26 min), the reaction was terminated by addition of 100 mM EDTA. After evaporation of ethyl acetate, 4.3 volumes of chloroform/methanol (5:8) were added to extract the product, and the mixture was filtered. To purify the product, 4.7 volumes of chloroform/0.15 M NaCl (3.7:1) were added to the filtrate (Comfurius & Zwaal, 1977). After centrifugation, the organic layer was taken out, and the purity of the product was assessed by TLC.

Cells. Blood was obtained by venipuncture from healthy adults and collected into tubes containing citric acid as anticoagulant. Erythrocytes were isolated by centrifugation and washed three times with 4 volumes of 150 mM NaCl and once with 138 mM NaCl, 5 mM KCl, 6.1 mM Na_2HPO_4, 1.4 mM NaH_2PO_4, 1 mM $MgSO_4$, and 5 mM glucose, pH 7.4 ($NaCl/P_i$). Cells were used within 5 h of being drawn. For incubations longer than 4 h, penicillin G (100 μg/mL) and streptomycin (100 μg/mL) were added to retard bacterial growth.

Vesicle Preparation. Small unilamellar lipid vesicles were prepared by suspending ^{14}C- or ^{3}H-radiolabeled lipids (0.05 μCi/mL) in $NaCl/P_i$ and sonicating the suspension to clarity in a bath sonicator. In the preparation of [^{3}H]DLPS vesicles, Mg^{2+} was omitted from $NaCl/P_i$ to avoid PS aggregation.

Cell Labeling. Sonicated vesicle suspensions of ^{14}C- or ^{3}H-radiolabeled lipids were incubated with cells [50% hematocrit (HCT)] at 37 °C for lengths of time sufficient to allow quantitative incorporation of the lipids into the cell membranes. In other experiments, endogenous lipids were labeled with [^{32}P]P_i by incubating in 5 volumes of 5 mM glucose–K^+/HEPES buffer (130 mM KCl, 20 mM HEPES, 2 mM $MgSO_4$, pH 7.4) containing 30 μCi/mL of [^{32}P]H_3PO_4. After 5-h incubation at 37 °C, cells were washed three times with K^+/HEPES buffer to remove excess [^{32}P]H_3PO_4.

Ca^{2+} Crenation and Repletion. Cells were washed twice with K^+/HEPES buffer to remove phosphate. Ca^{2+} crenation was accomplished by incubating cells (20% HCT) with various concentrations of Ca^{2+} and the cation ionophore A23187 at 37 °C. A23187 was added in ethanol/dimethyl sulfoxide (95:5 v/v) to yield a final concentration of 5 μM [ethanol concentration <1% (v/v)]. Ca^{2+} treatment was carried out in KCl medium to prevent K^+ efflux and cell shrinkage, and to diminish microvesiculation (Gardos et al., 1976; Allan & Thomas, 1981). Control cells were treated with the same concentration of the ionophore without Ca^{2+}. To convert Ca^{2+}-crenated cells to discocytes (repletion), cells were washed twice with 4 mM EGTA at 5% HCT. Cells (5% HCT) were then reincubated in supplemented K^+/HEPES buffer (K^+/HEPES buffer plus 10 mM inosine, 10 mM glucose, and 1 mM adenosine) for 15–30 min at 37 °C. In some experiments, Ca^{2+}-crenated cells were washed with EGTA at 0 °C and then treated with 0.1 mM sodium orthovanadate for 10 min at 37 °C before incubation in supplemented K^+/HEPES buffer containing 0.1 mM vanadate.

Extraction of Incorporated Radiolabeled Lipids by BSA. BSA was added to cells containing ^{14}C- or ^{3}H-radiolabeled lipids to yield a final concentration of 10–20% (w/v) at 5% HCT. After 20-min incubation at room temperature, cells were separated from the supernatant by centrifugation and washed twice with K^+/HEPES buffer to remove residual BSA. The fraction of radiolabel remaining in cells after this treatment was determined by liquid scintillation counting, and the difference between this value and the total lipid label was expressed as outer monolayer lipid.

OAG and Palmitic Acid Treatment. OAG and palmitic acid were added to metabolically depleted cells. Metabolic depletion was induced by incubating cells at 20% HCT with K^+/HEPES plus 10 mM inosine and 6 mM iodoacetamide. To ATP-depleted cells was added OAG in ethanol, to yield a final concentration of 0.5 mM [ethanol concentration 1% (v/v)], followed by washing to remove ethanol. This procedure was repeated five times to achieve incorporation of OAG in an amount in excess of the diacylglycerol found in Ca^{2+}-treated cells. Micellar palmitic acid (200 μM) was added to metabolically depleted cells at 50% HCT, and the cell suspension was incubated for 30 min at 37 °C. This treatment introduced a quantity of palmitate equal to 5.7% of total membrane lipid. Since both OAG and fatty acids flip rapidly ($t_{1/2} \sim 1$ min) across lipid bilayers, these treatments result in uniform distribution of both species in both membrane monolayers.

Analysis of Membrane Skeleton Proteins. Control, Ca^{2+}-crenated, and repleted cells were lysed at 4 °C in lysing buffer (5 mM Tris, 1 mM EDTA, pH 8) containing 50 μg/mL phenylmethanesulfonyl fluoride. The lysate was centrifuged at 12000*g* for 20 min, at 4 °C, and pelleted membranes were washed three times in lysing buffer until supernatants were free of detectable hemoglobin. Membrane samples were prepared for SDS gel electrophoresis as described (Huestis & Newton, 1986) and subjected to electrophoresis using 10% polyacrylamide gels (Ames, 1974). Gels were stained with

Coomassie brilliant blue R-250, and densitometry was performed by QuantiScan (Biosoft).

Assays. (A) Morphology. Erythrocytes were fixed in K^+/HEPES buffer containing 1% glutaraldehyde (pH 7.4). Cells were examined by light microscopy at a magnification of 500. Echinocytes were assigned morphology scores of +1 to +5 on the basis of Bessis's nomenclature (Bessis, 1973; Ferrell & Huestis, 1984). Discocytes were assigned a score of 0, and stomatocytes, scores of –1 to –4 (Daleke & Huestis, 1985). The average score for a field of 100 cells was defined as morphological index (MI) (Fujii et al., 1979). The MI values shown in the figures represent results of duplicate samples, counted twice. Where absent in figures, error bars were smaller than symbol size.

(B) ^{32}P-Labeled Phosphoinositides. Lipids were isolated and separated according to a previously published method (Ferrell & Huestis, 1984). Briefly, aliquots of frozen cell suspensions (100–250 μL) were lysed in 1 mL of ice-cold Tris/EDTA (10 mM Tris, 2 mM EDTA, pH 7.4) and centrifuged for 10 min at 12000*g*. The membranes were washed twice in Tris/EDTA, and lipids were extracted with 100:50:1 (v/v) methanol/chloroform/concentrated HCl (1.8 mL) followed by water (0.6 mL) and chloroform (0.6 mL). Lipids were separated by TLC on 10 × 20 cm plates (silica gel HLF) and developed in 48:40:7:5 (v/v) methanol/chloroform/water/concentrated NH_3. Lipid spots were detected with iodine vapor. Radiolabeled phospholipids were detected by autoradiography and quantified by AMBIS Radioanalytic Imaging System (AMBIS Systems Inc., San Diego, CA).

(C) ATP. Trichloroacetic acid [12% (w/v)] was added to an equal volume of the cell suspension (40% HCT). The mixture was vortexed vigorously and incubated on ice for 5–10 min. After centrifugation, aliquots of the supernatant were assayed for ATP using the Sigma ATP Diagnostics Kit (procedure no. 366-UV).

(D) Scintillation Counting. Cell pellets containing ^{14}C- or ^3H-radiolabeled lipids were solubilized by 10% Triton X-100. Samples were bleached by adding 10 volumes of 30% H_2O_2 and heating at 60–80 °C for 6–12 h (Daleke & Huestis, 1989). Bleached samples were suspended in EcoLite (ICN) and counted with a scintillation counter (Model LS-3801; Beckman Instruments).

RESULTS

Ca^{2+}-Induced Cell Crenation and Shape Recovery. Erythrocytes were treated with Ca^{2+} in the presence of A23187, a process known to elevate cytosolic Ca^{2+} (Scarpa et al., 1972; Lew & Garcia-Sancho, 1989). Cells incubated with Ca^{2+} and A23187 at 37 °C quickly converted to echinocytes of generally uniform morphology (Figure 1). The extent of crenation depended on the concentrations of Ca^{2+} and A23187 and the incubation time. The conditions employed (high-K^+ medium with 5 μM ionophore for 30 min) were designed to minimize membrane loss through budding (Allan & Thomas, 1981).

Ca^{2+}-induced cell crenation was reversible: after removal of the cation by EGTA, crenated cells incubated with nutrients at 37 °C recovered discoid shape within 15–30 min (Figure 1). The more severely echinocytic samples eventually developed slightly stomatocytic morphology during repletion.

Cytoskeletal Proteolysis in Ca^{2+}-Crenated and Recovered Cells. Elevated cytosolic Ca^{2+} in erythrocytes results in activation of an endogenous protease that cleaves the cytoskeletal proteins band 2.1 and band 4.1 (Allen & Cadman,

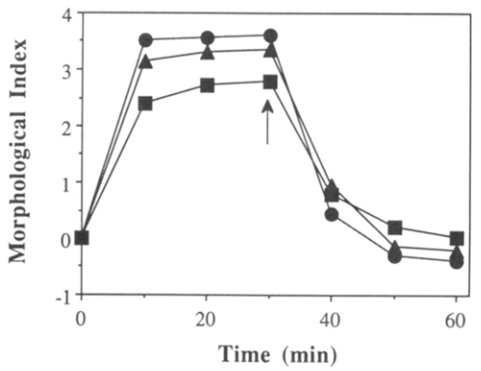

FIGURE 1: Calcium-induced cell crenation and reversal from crenation. Erythrocytes (20% HCT) in K^+/HEPES buffer were crenated by incubating with 0.2 mM (■), 0.5 mM (▲), and 1 mM (●) Ca^{2+} in the presence of ionophore A23187 (5 μM). After incubation for 30 min at 37 °C (arrow), cells were repleted by washing with EGTA and incubated in supplemented K^+/HEPES buffer (5% HCT) for 30 min.

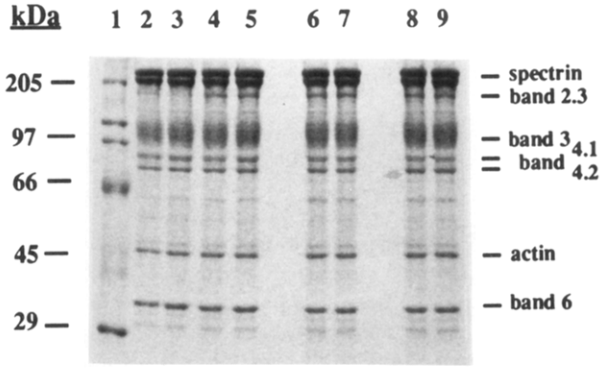

FIGURE 2: SDS gel electrophoresis of membrane proteins from Ca^{2+}-crenated and recovered cells. Cell crenation and repletion were conducted as described in the Figure 1 legend. Cells were treated with 0 (lane 2), 0.2 mM (lane 4), 0.5 mM (lane 6), and 1 mM Ca^{2+} (lane 8) for 30 min at 37 °C. Membranes from these samples after shape recovery are shown in lanes 3, 5, 7, and 9, respectively. Lane 1: Molecular weight standards.

1979; Allan & Thomas, 1981; Whatmore et al., 1992) and a transglutaminase which catalyzes cross-linking of membrane proteins (Anderson et al., 1977; Lorand et al., 1987). The role of cytoskeleton integrity in Ca^{2+}-induced reversible shape change was examined. Polyacrylamide gel electrophoresis of membranes from Ca^{2+}-crenated cells showed a significant increase in the intensity of band 2.3, a degradation product of band 2.1 (Figure 2). Densitometry analysis of the gel revealed a decrease in band 4.1 (to 85.96% of control protein) in cells loaded with 1 mM Ca^{2+}, consistent with earlier reports that degradation of this protein occurs only at high Ca^{2+} concentrations (Allan & Thomas, 1981; Chandra et al., 1987). When crenated cells recovered discoid shape upon incubation with nutrients, protein staining patterns did not change (Figure 2); thus, the integrity of these two proteins is not required for shape recovery from Ca^{2+} crenation. Formation of high-molecular-weight protein aggregates was not observed at the Ca^{2+} concentrations tested, indicating that activation of transglutaminase is not at play in Ca^{2+}-induced shape changes.

Phosphoinositide Degradation in Ca^{2+}-Crenated and Recovered Cells. The involvement of phosphoinositides in mediating Ca^{2+}-induced reversible shape change was examined. Erythrocytes incubated with [^{32}P]P_i for 5 h incorporated the radiolabel into PIP_2, PIP, and PA as reported (Allan & Michell, 1978; Ferrell & Huestis, 1984). When ^{32}P-labeled cells were crenated in buffer containing A23187 and various concentrations of Ca^{2+}, 60–80% of PIP and 50–75% of PIP_2

Table 1: Percent (%) of Radioactivity in PIP and PIP_2[a]

	PIP (%)		PIP_2 (%)	
Ca (mM)	crenated[b]	repleted[c]	crenated	repleted
0	100[d]	100[d]	100[d]	100[d]
0.2	47.00 ± 9.70	nd[e]	49.65 ± 1.85	nd
0.5	17.80 ± 3.10	17.65 ± 4.45	19.35 ± 4.65	24.30 ± 2.80
1.0	19.68 ± 2.43	23.55 ± 0.86	23.67 ± 1.25	26.07 ± 3.51

[a] Numbers are means ± standard deviation for triplicate assays. [b] ^{32}P-Labeled cells (20% HCT) were incubated for 15 min at 37 °C in K^+/HEPES buffer containing 5 μM A23187 and various concentrations of calcium to crenate cells. [c] Crenated cells were washed with 4 mM EGTA and 0.5% BSA and incubated in supplemented K^+/HEPES for 30 min at 37 °C to induce reversion to discocytes. [d] Membrane lipids from crenated and repleted cells were extracted from lysed cells and separated by TLC. The radioactivity of PIP and PIP_2 was quantitated using the AMBIS Radioanalytic Imaging System and normalized to control cells. [e] nd, not determined.

Table 2: Phospholipids in the Inner Monolayer (%) (SD)[a]

phospholipid	control	Ca^{2+}-crenated[b]	repleted[c]
[^{3}H]DLPS	94.47 ± 2.30	76.45 ± 1.91	94.15 ± 0.55
[^{14}C]DLPE	93.05 ± 0.34	82.82 ± 1.42	79.65 ± 0.06
[^{14}C]DLPC	12.31 ± 2.59	25.70 ± 4.18	26.91 ± 4.71
PIP	100[d]	17.80 ± 3.10	17.65 ± 4.45
PIP_2	100[d]	19.35 ± 4.65	24.30 ± 2.80

[a] Numbers are means ± standard deviation for triplicate assays. [b] Crenation was induced by incubating cells with 0.5 mM Ca^{2+} and 5 μM A23187 for 30 min at 37 °C. [c] See Figure 1 legend. [d] Radioactivity of PIP and PIP_2 was normalized to 100% in control cells.

were degraded (Table 1). PIP and PIP_2 remained depleted in cells allowed to recover discoid shape (Table 1). Since the sole phosphate source in this experiment was the prelabeled cellular P_i/ATP pool, any resynthesis of these lipids would have been evident as increased radiolabel.

Distribution of Radiolabeled PS, PE, and PC in Ca^{2+}-Crenated and Repleted Cells. The transbilayer distribution of the major phospholipids in erythrocytes was monitored by BSA extraction of incorporated radiolabeled lipids. At high specific activities, lipids incorporate in quantities sufficient for reextraction assays, without having independent effects on cell morphology. Cells were incubated with [^{14}C]DLPC, [^{14}C]DLPE, or [^{3}H]DLPS vesicles for intervals sufficient to achieve quantitative incorporation (30, 90, and 360 min, respectively). At steady state, 90% of incorporated DLPC was accessible to reextraction, while 5% of DLPS and DLPE were similarly accessible (Table 2; Figure 3, 0 mM Ca^{2+}).

This transbilayer distribution of radiolabeled phospholipids altered markedly when cytosolic Ca^{2+} was raised. The fraction of PC accessible to reextraction decreased in Ca^{2+}-crenated cells, while PE and PS became more accessible (Figure 3, open symbols). Both the degree of such lipid randomization and the extent of cell crenation increased with increasing Ca^{2+} concentration. When Ca^{2+}-crenated cells were allowed to recover discoid shape, only PS recovered its original distribution; PE and PC remained randomized (Figure 3, closed symbols).

The changes in the distribution of PS, PE, PC, and polyphosphoinositides in Ca^{2+}-crenated and recovered discocytes are summarized in Table 2. Treatment of cells with 0.5 mM Ca^{2+} caused degradation of polyphosphoinositides and randomization of the major phospholipids. Upon repletion, only PS was resequestered in the inner monolayer; other phospholipids remained randomized (PE and PC) or degraded (PIP and PIP_2).

Effects of Vanadate on Cell Shape Recovery and Phospholipid Distribution. Vanadate inhibits the aminophospholipid translocase which catalyzes movement of PS and PE from the outer to the inner monolayer of the membrane (Seigneuret & Devaux, 1984; Daleke & Huestis, 1985; Tilley et al., 1986; Connor & Schroit, 1987; Devaux 1991, 1992). The relationship between the shape recovery and PS resequestration was explored by vanadate treatment of Ca^{2+}-crenated cells. Erythrocytes were incubated with 0.5 mM Ca^{2+}, yielding an average morphology of +3.48 (Figure 4a, sample B). Upon repletion, crenated cells converted to discocytes plus a few stage−1 stomatocytes (Figure 4a, sample C). This shape recovery was blocked completely by inclusion of vanadate in the repletion medium (Figure 4a, sample D).

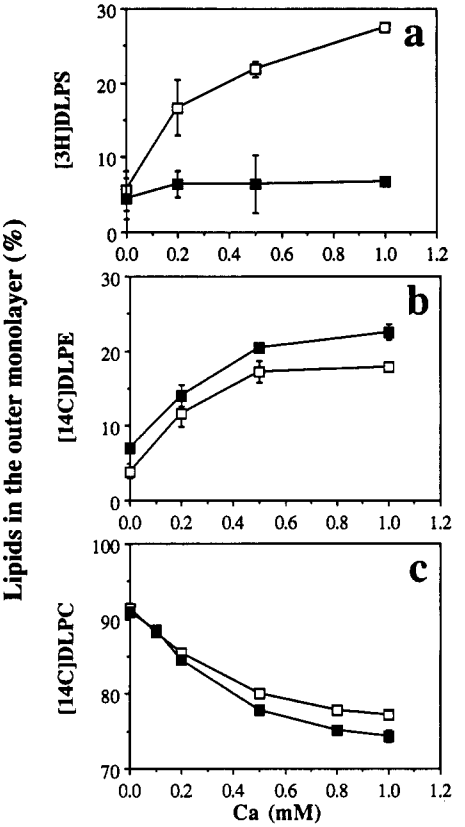

FIGURE 3: Extractable radiolabeled lipids in Ca^{2+}-crenated and recovered cells. Erythrocytes were labeled with (a) [^{3}H]DLPS, (b) [^{14}C]DLPE, and (c) [^{14}C]DLPC and then treated with various concentrations of Ca^{2+} and A23187. Ca^{2+}-crenated cells were repleted in supplemented K^+/HEPES as described in the Figure 1 legend. The distribution of radiolabeled lipids in Ca^{2+}-crenated (□) and in recovered (■) cells was determined by BSA extraction.

The inhibitory effect of vanadate was not due to inhibition of ATP synthesis (Figure 4b). Ca^{2+} treatment depleted ATP to about 6% of its original level (Figure 4b, sample B), in accordance with earlier reports (Allan et al., 1976a,b; Chandra et al., 1987; Lew & Garcia-Sancho, 1989). After 30-min incubation of cells with nutrients, ATP levels rose to 25% (Figure 4b, sample C) and 41% (Figure 4b, sample D), in the absence and presence of 0.1 mM vanadate, respectively. Thus, vanadate-treated cells regained more ATP during the repletion.

The distribution of phospholipids during the shape recovery of vanadate-treated cells was investigated by BSA extraction of incorporated phospholipids. Control cells prelabeled with [^{3}H]DLPS or [^{14}C]DLPC contained 85% of PC and 5% of PS as extractable (outer monolayer) fractions (Figure 5, sample A). In Ca^{2+}-crenated cells (MI = +3.48), 23% of PS was extractable (Figure 5a, sample B), while the fraction of extractable PC declined to 70% (Figure 5b, sample B). In the absence of vanadate, crenated cells recovered discoid shape

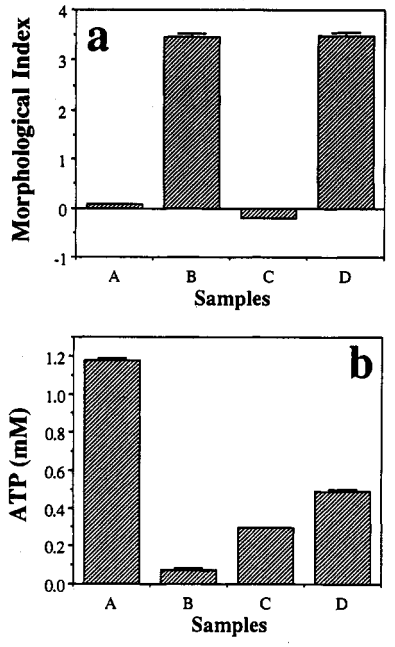

FIGURE 4: Effects of vanadate on (a) cell shape recovery, and (b) ATP levels, of Ca^{2+}-crenated cells. Control cells (sample A) were treated with 0.5 mM Ca^{2+} for 30 min at 37 °C (sample B) and then repleted as in Figure 1 (sample C), or repleted in the presence of 0.1 mM vanadate (sample D).

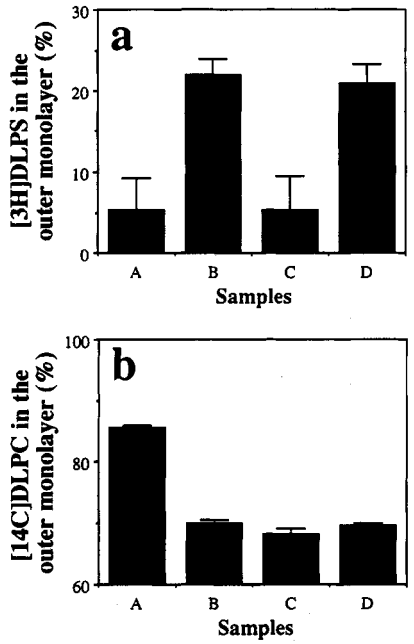

FIGURE 5: Effects of vanadate on distribution of radiolabeled lipids during shape recovery. Erythrocytes labeled with (a) [^{3}H]DLPS and (b) [^{14}C]DLPC were treated as in Figure 4. Cells are control (sample A), Ca^{2+}-crenated (sample B), repleted (sample C), and repleted in the presence of 0.1 mM vanadate (sample D).

with resequestration of PS in the inner monolayer (Figure 5a, sample C). In the presence of vanadate, resequestration of PS was inhibited (Figure 5a, sample D). This inhibition of PS resequestration coincided with the persistency of echinocytic shape: cells crenated to an MI of +3.48 retained a morphology of +3.50 after repletion in the presence of vanadate (Figure 4a, samples B and D). The distribution of PC was not affected by vanadate (Figure 5b, samples C and D).

Reversal of Vanadate Effects. The correlation between PS resequestration and shape recovery from Ca^{2+} crenation was examined further by reversal of the vanadate effect.

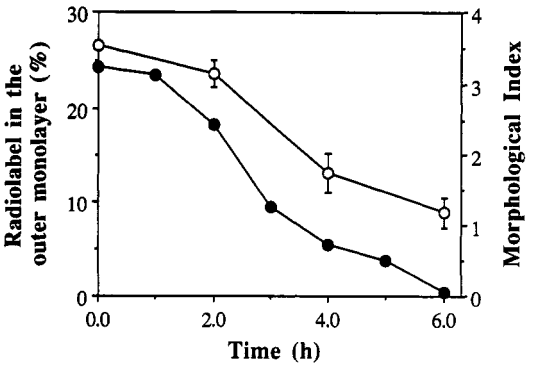

FIGURE 6: Reversibility of vanadate inhibition. Erythrocytes labeled with [^{3}H]DLPS were treated with 0.5 mM Ca^{2+} in the presence of A23187, washed with EGTA, and repleted in the presence of 0.1 mM vanadate for 30 min at 37 °C. Cells were then washed extensively and incubated in supplemented K^+/HEPES buffer, and shape change (●) and [^{3}H]DLPS distribution (○) were monitored.

Erythrocytes prelabeled with [^{3}H]DLPS were crenated by incubation with 0.5 mM Ca^{2+} plus ionophore. After removal of Ca^{2+} by EGTA, repletion was carried out in the presence of 0.1 mM vanadate for 30 min at 37 °C. Vanadate-treated cells remained crenated (Figure 6, time = 0 h). After extensive washing and subsequent incubation in vanadate-free supplemented buffer, crenated cells gradually converted to discocytes (Figure 6, closed symbols). This shape reversion coincided with gradual PS resequestration: 27% of [^{3}H]DLPS was accessible in echinocytic cells (time = 0 h), while 10% was extractable after cells recovered discoid shape (6 h) (Figure 6, open symbols). Thus effects of vanadate on both shape recovery and PS sequestration were reversible.

Effects of Metabolic Depletion, Diacylglycerol, and Fatty Acids on Phospholipid Distribution. As is shown in Figure 4b, elevated cytosolic Ca^{2+} depleted cellular ATP. The role of ATP depletion on phospholipid randomization was investigated in metabolically depleted cells. Metabolic depletion was initiated by incubating [^{3}H]DLPS- or [^{14}C]DLPC-labeled cells in iodoacetamide-containing buffer for 2 h at 37 °C, a process known to deplete ATP to <1% of control levels with little effect on cell shape (Feo & Mohandas, 1977). Back-extraction of incorporated radiolabeled lipids revealed that PC and PS distribution was similar in metabolically depleted and control cells (Figure 7, samples A and B). Thus, metabolic depletion alone did not cause phospholipid randomization.

Elevated intracellular Ca^{2+} produces DG by hydrolyzing polyphosphoinositides, and the resulting DG is quickly phosphorylated to yield PA in ATP-replete cells (Allan & Thomas, 1981). The role of elevated DG on phospholipid randomization was examined. OAG was added to radiolabeled cells which had been metabolically depleted to prevent OAG phosphorylation. OAG was introduced into cells by repeated ethanol injection. The amount incorporated was 3-fold greater than the endogenous level in Ca^{2+}-loaded cells, as verified by TLC. BSA extraction analysis showed that the distribution of [^{3}H]DLPS and [^{14}C]DLPC was similar in OAG-loaded cells and in controls (Figure 7, sample C), in contrast to Ca^{2+}-treated cells (Figure 7, sample D). These results indicate that the transient increase in DG produced by Ca^{2+}-activated phospholipase C is unlikely to cause lipid randomization.

Increased intracellular Ca^{2+} also activates a phospholipase A_2, which cleaves phospholipids into fatty acids and lysophospholipids. The role of fatty acids in reorganization of phospholipids was examined. Metabolically depleted cells were labeled with [^{14}C]DLPC and then allowed to incorporate palmitic acid in a quantity consistent with degradation of

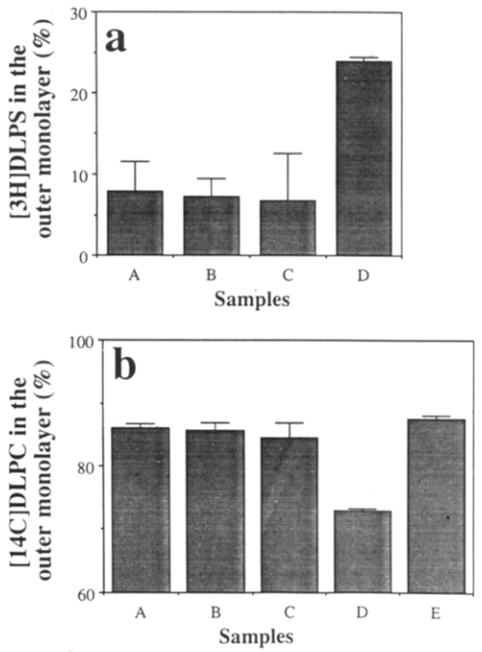

FIGURE 7: Effects of metabolic depletion, OAG, and palmitic acid on the distribution of radiolabeled lipids. Erythrocytes labeled with (a) [^{3}H]DLPS and (b) [^{14}C]DLPC were metabolically depleted in sugar-free buffer containing 10 mM inosine and 6 mM iodoacetamide for 2 h at 37 °C. ATP-depleted cells were then treated with OAG and palmitic acid as described in Materials and Methods. Samples are control (sample A), metabolically depleted (sample B), metabolically depleted and treated with OAG (sample C) or palmitic acid (panel b, sample E), and Ca^{2+}-treated (sample D) cells.

5.7% of native phospholipid (this amount of fatty acid is at least an order of magnitude greater than the observed content of Ca^{2+}-treated cells). [^{14}C]DLPC was equally accessible to BSA extraction in control and palmitate-treated samples (Figure 7b, samples A and E), indicating little fatty acid-induced lipid randomization.

DISCUSSION

Maintenance of lipid asymmetry may be important for normal circulation of erythrocytes; increased surface exposure of PS may serve as a signal for sequestration by the reticuloendothelial system (Schroit et al., 1985; Schlegel et al., 1985). Elevated cytosolic Ca^{2+} causes at least partial loss of PS asymmetry in human erythrocytes, as has been demonstrated independently by prothrombinase and phospholipase A_2 assays, which detect surface exposure of endogenous PS (Williamson et al., 1985; Comfurius et al., 1990a,b; Henseleit et al., 1990; Chandra et al., 1987; Zwaal et al., 1993), and by back-extraction of incorporated spin- or fluorescent-labeled aminophospholipid analogs (Williamson et al., 1992; Connor et al., 1990). Conflicting results have been reported regarding the effects of Ca^{2+} on PC disposition: while investigations using spin- or fluorescent-labeled PC or radiolabeled lysoPC have revealed an accelerated flip of PC to the membrane inner monolayer (Williamson et al., 1992; Henseleit et al., 1990), phospholipase A_2 assays fail to detect such change (Chandra et al., 1987; Henseleit et al., 1990). In the present study, radiolabeled phospholipids were incorporated into cells, and their transbilayer distribution was assessed by measuring their accessibility to reextraction by exogenous BSA. Lipids having high specific activity may be incorporated into cells in amounts sufficient for the extraction assay without independent effects on cell morphology. The distribution of these lipids in control cells (Table 2) is similar to that of the endogenous phospholipid homologs. Reextraction and scintillation counting of the labeled lipids is a sensitive and reliable monitor of their transbilayer distribution in the intact cell (Daleke & Huestis, 1989; Morrot et al., 1989; Connor et al., 1990; Henseleit et al., 1990; Schroit & Zwaal, 1991).

Cell Shape Changes and Bilayer Balance. As previous reports have shown, Ca^{2+} influx in erythrocytes induces both polyphosphoinositide degradation and phospholipid randomization; PS and PE are exposed in the membrane outer leaflet, PC flips to the membrane inner leaflet, and the inner monolayer components PIP and PIP_2 are depleted. The net morphological effect of the major phospholipid redistribution is not readily predictable; a one-to-one exchange of inner and outer monolayer components would produce no change in bilayer balance, but the available methods for detecting qualitative distribution changes are insufficient to determine the exact stoichiometry of the lipid scrambling. However, an earlier analysis (Ferrell & Huestis, 1984) indicated that phosphoinositide degradation is sufficient to produce the bilayer imbalance associated with crenation. Thus, it is not necessary to invoke differential scrambling of inner and outer monolayer lipids to produce the observed morphology change.

Ca^{2+}-crenated cells recover discoid shape on removal of Ca^{2+} and supplementation with nutrients (Figure 1). This shape reversion cannot be attributed to regeneration of the phosphoinositides from DG or PA, nor to phosphorylation of a membrane PI pool (Anderson, 1989) not affected by the calcium treatment, since PIP and PIP_2 populations do not increase significantly as cells replete (Table 1). The observed recovery to discoid shape is, however, consistent with differential redistribution of the major phospholipid classes, with preferential transit of outer monolayer components to the inner monolayer. A similar resequestration of exposed PS has been observed in cells whose lipids were randomized by amphipath treatment (Schrier et al., 1992). In summary, these findings suggest that crenation and reversal to discoid shape proceed by different molecular mechanisms.

Cell Shape Reversal and Recovery of PS Asymmetry. Consistent with this suggestion, cell shape reversal from Ca^{2+} crenation is found to correlate with PS retransit to the membrane inner monolayer (Figure 3). No similar recovery of transbilayer asymmetry is detected for the normal outer monolayer choline lipid, or for PE. Activity of the aminophospholipid translocator is necessary for both PS sequestration and shape recovery, since both are abolished by the translocase inhibitor vanadate (Figures 4 and 5). The correlation between PS resequestration and shape recovery is supported by the reversibility of both vanadate effects: upon removal of extracellular vanadate, cells recover both discoid shape and PS inaccessibility at similar slow rates (Figure 6). The duration of these changes (6 h) may reflect a slow conversion of vanadate to vanadyl by cytosolic reductants (Heinz et al., 1982); vanadyl ion (VO^{2+}) does not inhibit the PS translocase (Bitbol et al., 1987).

The biochemical characteristics of the aminophospholipid translocase are consistent with its proposed role in Ca^{2+}-mediated shape changes. The translocase is inactivated by Ca^{2+}, both directly (Bitbol et al., 1987; Zachowski et al., 1986) and as a consequence of the attendant ATP depletion (Devaux, 1991, 1992; Zwaal et al., 1993); thus, it would be incapable of relocating outer monolayer PS and PE while the cation is present. Removal of calcium and nutrient supplementation produces partial recovery of ATP (to 25% of normal), which is sufficient to fuel translocation of PS (Daleke & Huestis, 1985; Zachowski et al., 1986). As is indicated by the effects

of vanadate (Figure 4), ATP regeneration per se is not sufficient to initiate shape recovery, again consistent with a mechanistic link to the translocater.

Previous studies showed that, after removal of Ca^{2+} by EGTA, newly incorporated phospholipid probes assume their normal distribution (Henseleit et al., 1990; Williamson et al., 1992). While these studies convincingly demonstrate that Ca^{2+}-mediated membrane perturbation is a transient event, the claim that Ca^{2+}-induced lipid randomization is reversible could be misleading in that these studies did not reveal the eventual fate of the lipids randomized by the perturbation. The present results show that, among randomized phospholipids, PS is the only lipid restored to near-normal distribution upon Ca^{2+} removal and cell repletion. The lack of redistribution of PC probably is due to the absence of an active transporter that can facilitate the movement of PC across the bilayer. Failure to detect any PE resequestration may reflect the fact that the recovered ATP level (25%) is not sufficient to allow the translocase to transport PE efficiently (Devaux, 1991). Competition experiments demonstrated that translocation of PE is generally less efficient than is found with PS: the apparent affinity of the translocase for PE is approximately 10-fold lower than for PS (Zachowski et al., 1986; Beleznay et al., 1993), and the ratio of inward to outward translocation rates (k_i/k_o) is ~19 for spin-labeled PS, versus ~6.7 for spin-labeled PE (Bitbol & Devaux, 1988).

Effect of Cytoskeletal Degradation on Cell Shape Changes and PS Asymmetry. Elevated cytoplasmic Ca^{2+} inevitably causes degradation of band 2.1 (ankyrin) and, to a lesser extent, band 4.1. As both proteins have been shown to play pivotal roles in modulating membrane–cytoskeleton interactions, Ca^{2+}-induced loss of phospholipid asymmetry and cell crenation have been attributed to destabilization of the cytoskeleton and weakened cytoskeleton–phospholipid interaction upon 2.1 and 4.1 proteolysis (Chandra et al., 1987). The present work indicates that degradation of these proteins does not prevent recovery of either discoid morphology or PS asymmetry (Figure 2). These results argue against the importance of cytoskeletal integrity in maintenance of PS asymmetry and in inducing cell crenation. Consistent with these observations, recovery of PS asymmetry upon Ca^{2+} removal reportedly does not require inhibition of Ca^{2+}-dependent protease (Comfurius et al., 1990b), and ankyrin may not be essential for the maintenance of discoid morphology (Whatmore et al., 1992).

Possible Mechanisms for Ca^{2+}-Induced Lipid Randomization. Several possible mechanisms for Ca^{2+}-induced lipid randomization were examined. Although Ca^{2+} strongly inhibits the aminophospholipid translocase, the rapid surface exposure of PS and PE in Ca^{2+}-treated cells cannot be attributed solely to inactivation of the translocase, since the passive transverse movement of endogenous lipids proceeds at much slower rates (Daleke & Huestis, 1985; Bitbol & Devaux, 1988; Zachowski & Devaux, 1989; Schroit & Zwaal, 1991); additionally, Ca^{2+}-induced loss of asymmetry in erythrocyte ghosts is reported to be independent of the translocase (Verhoven et al., 1992). Ca^{2+}-induced microvesiculation is unlikely to play a major role in lipid reorientation, since hemoglobin release under our conditions (K^+ medium) was less than 1% with the highest Ca^{2+} concentration tested (1 mM). Ca^{2+} influx causes ATP depletion (Figure 4), but the depletion alone has no effect on the distribution of PC and PS (Figure 7), consistent with other reports showing no PS exposure or alteration of lipid asymmetry in ATP-depleted cells (Williamson et al., 1985; Tilley et al., 1986; Henseleit et al., 1990). Studies on lipid model membranes have shown that both DG and fatty acids perturb lipid bilayer by facilitating formation of inverted micelles (H_{II}) and membrane fusion (Epand, 1985; Siegel et al., 1989; Cunningham et al., 1989; De Boeck & Zidovetzki, 1989, 1992). Involvement of these two lipids in Ca^{2+}-induced lipid reorientation is unlikely, since direct loading of cells with the lipids does not alter the normal distribution of PC and PS (Figure 7).

Further studies will be required to fully understand the mechanism of Ca^{2+}-induced lipid scrambling. It is possible that the observed lipid reorganization might be mediated by direct interactions of Ca^{2+} with phospholipids (especially negatively charged ones) to form disordered domains that randomize proximal lipids. Studies on model membranes suggest that millimolar concentrations of Ca^{2+} increase the tendency of the negatively charged phospholipids to adopt nonbilayer organization (Tilcock et al., 1984; Mattai et al., 1989; Portis et al., 1979). Although the ionophore A23187 alone does not induce lipid randomization (as controls containing the ionophore have normal phospholipid distribution), the ionophore may facilitate formation of Ca^{2+}–phospholipid domains within the membrane bilayer.

ACKNOWLEDGMENT

We thank M. Moxness for synthesis of [^{3}H]DLPS and for help in the purification of [^{14}C]DLPE.

REFERENCES

Allan, D., & Michell, R. H. (1975) *Nature 258*, 348–349.
Allan, D., & Michell, R. H. (1978) *Biochim. Biophys. Acta 508*, 277–286.
Allen, D. W., & Cadman, S. (1979) *Biochim. Biophys. Acta 551*, 1–9.
Allan, D., & Thomas, P. (1981) *Biochem. J. 198*, 433–440.
Allan, D., Watts, R., & Michell, R. H. (1976a) *Biochem. J. 156*, 225–232.
Allan, D., Billah, M. M., Finean, J. B., & Michell, R. H. (1976b) *Nature 261*, 58–60.
Ames, G. F. L. (1974) *J. Biol. Chem. 249*, 634–644.
Anderson, D. R., Davus, J. L., & Carraway, K. L. (1977) *J. Biol. Chem. 252*, 6617–6623.
Anderson, R. A. (1989) in *Red Cell Membranes* (Agre, P., & Parker, J. C., Eds.) pp 187–236, Dekker, New York.
Anderson, R. A., & Lovrien, R. E. (1981) *Nature 292*, 158–161.
Beleznay, Z., Zachowski, A., Devaux, P. F., Navazo, M. P., & Ott, P. (1993) *Biochemistry 32*, 3146–3152.
Bessis, M. (1973) in *Red Cell Shape* (Bessis, M., Weed, R. I., & LeBlond, P. F., Eds.) pp 1–23, Springer Verlag, New York.
Bitbol, M., & Devaux, P. F. (1988) *Proc. Natl. Acad. Sci. U.S.A. 85*, 6783–6787.
Bitbol, M., Fellmann, A., Zachowski, A., & Devaux, P. F. (1987) *Biochim. Biophys. Acta 904*, 268–282.
Chandra, R., Joshi, P. C., Bajpai, V. K., & Gupta, C. M. (1987) *Biochim. Biophys. Acta 902*, 253–262.
Cohen, C. M., & Gascard, P. (1992) *Semin. Hematol. 29*, 244–292.
Comfurius, P., & Zwaal, R. F. A. (1977) *Biochim. Biophys. Acta 488*, 36–42.
Comfurius, P., Bevers, E. M., & Zwaal, R. F. A. (1990a) *J. Lipid Res. 31*, 1719–1721.
Comfurius, P., Senden, J. M. G., Tilly, R. H. L., Schroit, A. J., Bevers, E. M., & Zwaal, R. F. A. (1990b) *Biochim. Biophys. Acta 1026*, 153–160.
Connor, J., & Schroit, A. J. (1987) *Biochemistry 27*, 848–851.
Connor, J., Gillum, K., & Schroit, A. J. (1990) *Biochim. Biophys. Acta 1025*, 82–86.
Cunningham, B. A., Tsujita, T., & Brockman, H. L. (1989) *Biochemistry 28*, 32–40.

Daleke, D. L., & Huestis, W. H. (1985) *Biochemistry 24*, 5406–5416.
Daleke, D. L., & Huestis, W. H. (1989) *J. Cell Biol. 108*, 1375–1385.
De Boeck, H., & Zidovetzki, R. (1989) *Biochemistry 28*, 7439–7446.
De Boeck, H., & Zidovetzki, R. (1992) *Biochemistry 31*, 623–690.
Devaux, P. F. (1991) *Biochemistry 30*, 1163–1173.
Devaux, P. F. (1992) *Annu. Rev. Biophys. Biomol. Struct. 21*, 417–439.
Epand, R. M. (1985) *Biochemistry 24*, 7092–7095.
Feo, C., & Mohandas, N. (1977) *Nature 265*, 166–168.
Ferrell, J. E., & Huestis, W. H. (1982) *Biochim. Biophys. Acta 687*, 321–328.
Ferrell, J. E., & Huestis, W. H. (1984) *J. Cell Biol. 98*, 1992–1998.
Ferrell, J. E., Lee, K. J., & Huestis, W. H. (1985) *Biochemistry 24*, 2849–2857.
Fujii, T., Sato, T., Tamura, A., Wakatsuki, M., & Kanaho, Y. (1979) *Biochem. Pharmacol. 28*, 613–620.
Gardos, G., Lassen, U. V., & Pape, L. (1976) *Biochim. Biophys. Acta 448*, 599–606.
Heinz, A., Rubenstien, K. A., & Grantham, J. J. (1982) *J. Lab. Clin. Med. 100*, 593–612.
Henseleit, U., Plasa, G., & Haset, C. (1990) *Biochim. Biophys. Acta 1029*, 127–135.
Huestis, W. H., & Newton, A. C. (1986) *J. Biol. Chem. 261*, 16274–16278.
Juneja, L. R., Kazuoka, T., Yamane, T., & Shimizu, S. (1988) *Biochim. Biophys. Acta 960*, 334–341.
Kramer, R. M., Chegani, G. C., & Deykin, D. (1987) *Biochem. J. 248*, 779–783.
Lew, V. L., & Garcia-Sancho, J. (1989) *Methods Enzymol. 173*, 100–112.
Lorand, L., Barnes, N., Bruner-Lorand, J. A., Hawkins, M., & Michalska, M. (1987) *Biochemistry 26*, 308–313.
Mattai, J., Hauser, H., Demel, R. A., & Shipley, G. G. (1989) *Biochemistry 28*, 2322–2330.
Morrot, G., Herve, P., Zachowski, A., Fellmann, P., & Devaux, P. F. (1989) *Biochemistry 28*, 3456–3462.
Ponnappa, B. C., Greenquist, A. C., & Shohet, S. B. (1980) *Biochim. Biophys. Acta 598*, 494–501.
Portis, A., Newton, C., Pangborn, W., & Papahadjopoulos, D. (1979) *Biochemistry 18*, 780–789.
Raval, P. J., & Allan, D. (1985) *Biochem. J. 232*, 43–47.
Roelofsen, B, Op den Kamp, J. A. F., & van Deenen, L. L. M. (1987) *Biomed. Biochim. Acta 46*, S10–S13.
Scarpa, A., Baldassare, J., & Inesi, G. (1972) *J. Gen. Physiol. 60*, 735–749.
Schlegel, R. A., Prendergast, T. W., & Williamson, P. (1985) *J. Cell Physiol. 123*, 215–218.
Schrier, S. L., Zachowski, A., & Devaux, P. F. (1992) *Blood 79*, 782–786.
Schroit, A. J., & Zwaal, R. F. A. (1991) *Biochim. Biophys. Acta 1071*, 313–329.
Schroit, A. J., Madsen, J. W., & Tanaka, Y. (1985) *J. Biol. Chem. 260*, 5131–5138.
Seigneuret, M., & Devaux, P. F. (1984) *Proc. Natl. Acad. Sci. U.S.A. 81*, 3751–3755.
Sheetz, M. P., & Singer, S. J. (1974) *Proc. Natl. Acad. Sci. U.S.A. 71*, 4457–4461.
Siegel, D. P., Banschbach, J., Alford, D., Ellens, H., Lis, L. J., Quinn, P. J., Yeagle, P. L., & Bentz, J. (1989) *Biochemistry 28*, 3703–3709.
Sims, P., Wiedmer, T., Esmon, C., Weiss, H., & Shattil, S. (1989) *J. Biol. Chem. 264*, 17049–17057.
Stockton, G. W., Polnaszek, C. F., Leitch, L. C., Tulloch, A. P., & Smith, I. C. P. (1974) *Biochem. Biophys. Res. Commun. 60*, 844–850.
Tilcock, C. P. S., Bally, M. B., Farren, S. B., Cullis, P. R., & Gruner, S. M. (1984) *Biochemistry 23*, 2696–2703.
Tilley, L., Cribier, S., Roelofsen, B., Op den Kamp, J. A. F., & Van Deenen, L. L. M. (1986) *FEBS Lett. 194*, 21–27.
Verkleij, A. J., Zwaal, F. A. F., Roelofsen, B., Comfurius, P., Kastelijn, D., & van Deenen, L. L. M. (1973) *Biochim. Biophys. Acta 323*, 178–193.
Verhoven B., Schlegal, R. A., & Williamson, P. (1992) *Biochim. Biophys. Acta 1104*, 15–23.
Whatmore, J. L., Tang, E. K. Y., & Hickman, J. A. (1992) *Exp. Cell Res. 200*, 316–325.
White, J. G. (1974) *Am. J. Pathol. 77*, 507–518.
Williamson, P., Algarin, L., Bateman, J., Choe, H. R., & Schlegel, R. A. (1985) *J. Cell. Physiol. 123*, 209–214.
Williamson, P., Kulick, A., Zachowski, A., Schlegel, R. A., & Devaux, P. F. (1992) *Biochemistry 31*, 6355–6360.
Zachowski, A., Favre, E., Cribier, S., Herve, P., & Devaux, P. F. (1986) *Biochemistry 25*, 2585–2590.
Zwaal, R. F. A., Comfurius, P., & Bevers, E. M. (1993) *Biochem. Soc. Trans. 21*, 248–253.